УДК 548.57 Original paper

Low-frequency impedance spectroscopy of polymers and crystals with a hydrogen-bond network. Quantum collective excitations of nuclei in molecules

O.D. Novik¹, N.D. Gavrilova¹, O.V. Malyshkina²

¹M.V. Lomonosov Moscow State University, Moscow, Russia

²Tver State University, Tver, Russia

Olga.Malyshkina@mail.ru

DOI: 10.26456/pcascnn/2024.16.239

Abstract: In this work, we present the results of our studies of temperature-frequency behaviour of dielectric permittivity ε , conductivity σ , relaxation time τ_{μ} , thermodepolarisation currents j, and pirocurrents γ in hydrophilic polymers and crystals with a hydrogen-bond network OH...O in the ranges of 0,01–10⁷ Hz and 20-140°C. Analysis of the obtained data has revealed temperature anomalies of $\varepsilon(T)$, $\sigma(T)$, $\tau_{\mu}(T)$, j(T), and $\gamma(T)$ around «threshold» points at 20, 36, 50, 65, and 85°C, where the destruction of water clusters (and, if above 100°C, of water molecule itself) takes place, and thereby the release of deep traps, the change of the charge carriers $(H_3O^+, OH^-, \text{ etc.})$ composition and of their trajectories in volume are observed. In this study, we draw an analogy between the temperature behaviour of ε , σ , τ_{μ} , j, and y in «threshold» points having a characteristic single resonance peak and the dipole resonance of photoabsorption in clusters of Ag, Mg, and Sm metals, which is manifested in the broadening of resonance, single peak splitting, and in the formation of single-domain ATGS+ Cr^{3+} crystal (0,06 wt.% Cr). We also discuss a possible onset of collective nuclear excitements during irradiation with photons or an onset of internal electrical displacement field E_{dp} in a sudden sample cooling or warming. The entanglement of photons by polarization is also considered.

Keywords: giant dipole resonance, discrete energy levels of double-well potential, dielectric permittivity and conductivity, coherent collective excitements of nuclei, splitting of resonance maxima of ε , σ and of conductivity relaxation time τ_{μ} , spin probability field.

1. Introduction

Impedance spectroscopy is a set of physical methods suitable for the observation of physico-chemical properties of materials. As we suppose, a characteristic feature of the temperature behaviour of such properties as dielectric permittivity ε , electrical conductivity σ , vector of spontaneous electrical polarisation \mathbf{P}_{s} , thermodepolarisation currents (TDC) j, and pyroelectric currents γ is the coincidence of the temperatures T_{max} of the anomalies of these parameters with the corresponding energy jumps of the double-well potential under the heating stage. For a great number of solid samples of ferroelectrics, monocrystals, and polymers containing water or hydrogen bonds OH...O, the dependences $\varepsilon(T)$, $\sigma(T)$, $\gamma(T)$, j(T) and the temperature dependence of conductivity relaxation time $\tau_{\mu}(T)$ were studied. One of the principal manifestations of quantum physical behaviour of these materials is that, in the low frequency range ($f \approx 0.07 - 10^4$ Hz) and for temperatures from -90 to 200°C, there are temperature points where parameters ε , σ , γ and j rise

anomalously by one or two orders of magnitude. These properties reflect the behaviour of the dipole moments of molecules, as well as of protons and neutrons in nuclei, and of the whole sample under the order—disorder transition. In this work, a number of materials were studied that contain an *OH...O* hydrogen-bond network in a lattice of molecules composing crystalline hydrates, hydrogels, polymers and biopolymers with some «matrix-water» systems.

The structure of water can be represented as a complex three-dimensional dynamic hydrogen-bond network, which is continuously rearranging due to the heat motion of particles [1-4]. Each water molecule can be free or can be a part of a cluster composed of 2-6 hydrogen bonds, from which bigger globules are formed, which a rearrange around threshold points at 4, 20, 36, 46, 65, and 78°C, according to discrete energy spectra observed under stage heating (see fig. 1) [5].

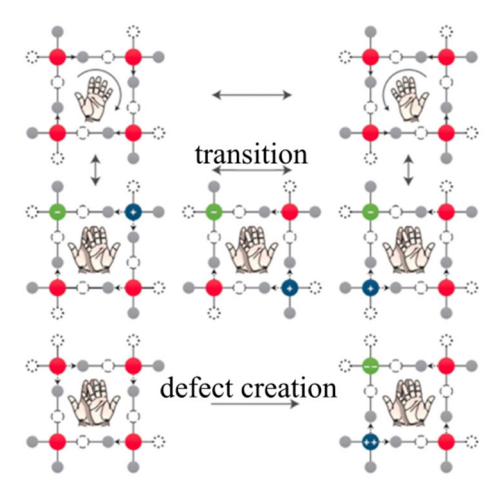


Fig. 1. Schemes of various proton transitions in chiral and achiral tetrahedral clusters of water [2].

From the point of view of quantum electrodynamics, the low-frequency $(10^{-1}-10^3 \text{ Hz})$ impedance of ferroelectrics with a network of H-bonds describes the movements of large molecules and various atomic nuclei [2, 5-8].

Many laboratories around the world are engaged in the search for new dielectric materials for microcircuits, microwave, IR and ultra-low frequency radiation sensors, as well as in the studies of the effects of fine impurities in solutions, biological fluids, hydrogels, crystalline hydrates and biopolymers. The presence of a network of OH...O bonds can cause a correlated and coherent response to changes of external and internal electric displacement fields E_{dp} , for example, under temperature changes or under irradiation with electromagnetic waves. Waves of the optical range are usually implied [2, 5-9]. Impedance spectra are often no less informative for applied materials science.

The rapid development of quantum theory in physics has contributed to a deeper understanding of electrophysical temperature experiments in a wide range of materials containing dipole sublattices of the most common crystalline hydrates, hydrogels, polymers, including biopolymers and cross-linked composite materials.

In our experimental studies of temperature anomalies in a wide range of 4 to 460 K, we often confirmed the presence of singular points, where such parameters of samples as dielectric permittivity $\varepsilon(T)$, conductivity $\sigma(T)$, thermodepolarization currents j(T), and pyroelectric coefficient $\gamma(T)$ show anomalous increases at T_{max} or a structural phase transition at the Curie point T_c . These manifestations are most prominent in crystals of triglycine tellurate $(NH_2CH_2COOH)_3 \cdot H_6TeO_6$ (TGTel), triglycine sulphate $(NH_2CH_2COOH)_3 \cdot H_2SO_4$ (TGS), potassium dihydrogen phosphate (KDP) isomorphs, alum; holmium, yttrium and erbium formats, acid sulfates and tartrates of potassium-sodium, lithium-thallium and in a number of hydrophilic polymers such as polyacrylic acid (PAA), its sodium salt (PANa) and polyvinylidene fluoride with trifluoroethylene (PVDF-TrFE) [10-19]. For the obtained experimental dependences $\varepsilon(T)$, $\tau_u(T)$, and $\sigma(T)$, some anomalous phenomena («plateau» before T_c , doubled peaks in $\varepsilon(T)$, $\sigma(T)$, and $\tau_u(T)$ at «threshold» points), as well as peak broadening [10-19] and growth of domainless crystals of triglycine sulphate (TGS), doped with α -alanine (0,05 wt. %) and chromium (0,06 wt. %), are of particular interest. TGS crystals doped with L-α-alanine (ATGS) doped with Cr^{3+} do not present any pronounced peak at T_c , only wide blurred peaks in $\varepsilon(T)$, $\gamma(T)$ are observed instead; P_s exists up to ~130°C, which is 80°C above the point of T_c for the order-disorder transition (T_c 49,7°C) in pure crystals, where the spontaneous polarization P_s vanishes; the value of $\gamma(T)$ decreases to zero, and ε and σ [4] decrease to small values.

In this connection, the following questions arise:

- Why does TGS growing from an aqueous solution with additions of L, α -alanine and chromium (with the formation of chelate complexes) forms single-domain crystals on a single-domain seed?
- Why, under stage heating in potassium dihydrogen phosphate and all its isomorphs, below the Curie point, does ε start to rise at a temperature which is 20 C below T_c ; why is this followed by a plateau of $\varepsilon(T)$ and again by a weak peak at the Curie point; and why, at frequencies of 1 kHz, this phaenomenon becomes more pronounced than at a frequency of 10 kHz, with a shift to the right from T_c ?

According to modern concepts, several groups of energy levels can exist in a complex solid-phase sample: separate levels for protons and neutrons, nuclei, all particles of the subsystem; separate levels for groups of atoms (for example, the K-P framework in KDP and the network of OH...O bonds); and

separate levels for the entire system of the crystal and the sublattice inserted into it. Even in the *OH...O* systems of water or in *OH...O* of hydrogen-bond network there are more than three groups of hydrogen bonds.

2. Methods and materials

The measurements were carried out using dielectric spectroscopy and thermally stimulated depolarization currents (TSDC) methods. Dielectric measurements were carried out using a P551 AC bridge (20-10-4 Hz) and a Novocontrol Concept 40 broadband dielectric spectrometer (10⁴–10⁷ Hz). TSDC j(T) were measured by the static method (with temperature stabilization better than 0,01) using a VA-J-51 electrometer with current recorded on a selfrecording potentiometer. One group of samples were single crystals containing water molecules or H-bonds of the same length in the structure. Four of them were ferroelectric TGS and its structure analogue TGTel, diglycine nitrate (NH₂CH₂COOH)₃·HNO₃ (DGN). Two other crystals were crystallohydrates: holmium formate $Ho(HCOO)_3 \cdot 2H_2O$ (Ho formate). The samples from this group were plane-parallel plates, on previously prepared (polished) opposite surfaces of which silver electrodes were applied. The second group of objects included polymeric materials, which adsorbed water molecules during preparation of the samples. After polymerization of vinylidene fluoride - trifluoroethylene (PVDF/TrFE) 70/30 copolymer, the copolymer films were annealed at 110°C and then immediately immersed in water [17], so water molecules were able to enter the surface layer and bind to polymer molecules. The samples of lightly crosslinked polyampholytes (PAA and PANa [18]) were obtained by «soft» drying of corresponding hydrogels. The samples of hydrophilic polymer materials PAA and PA-Na were prepared by compressing a powder of the corresponding polymer to a tablet [14]. Silver paste was used to prepare the electrodes for this group of samples. Conductivity relaxation time $\tau_{\mu}(T)$ was calculated from the $\varepsilon(T)$ and $\sigma(T)$ data.

3. Results and discussion

The article [7] discusses theoretical and experimental studies involving the concept of the giant dipole resonance as a collective coherent excitation of nuclei, in the framework of which all nucleons of the nucleus are involved in oscillations, and the movement of all protons relative to all neutrons generates electrical dipole excitation (GDR – giant dipole resonance). This is a universal nuclear phenomenon – a transition to an excited state after the absorption of photons by atomic nuclei and free nucleons as a reaction to electromagnetic radiation. The magnitude of isospin splitting increases with an increase of the neutron excess (n-z) > 0. Dielectric giant dipole resonance is also observed in

systems such as metal clusters, fullerenes and non-nuclear systems. The main theoretical approaches used to describe GDR in these systems are borrowed from nuclear physics [5, 7-9] (see fig. 2).

In [7, 8], formulae are given for the dipole moment d emerging in the nucleus exposed to a homogeneous external field. The average energy of dipole transitions is given by the formula:

$$\frac{\sum_{n} |d_{on}|/(E_{n}-E_{o})}{\sum_{n} (E_{n}-E_{o})|d_{on}|^{2}} = \left(\frac{1}{E}\right)^{2},$$

where d_{on} is the static dipole moment acquired by the nucleus during the transition from the ground state with energy E_o to the excited state with energy E_n .

The denominator is obtained using the classical formula $\left[2\pi^2e^2/(mc)\right]z$, where m is the mass of nucleons, and n, z – neutron and proton counts, respectively.

According to [8], the mean energy of dipole excitations E for heavy nuclei is:

$$E = \sqrt{40 \frac{nz}{A^2}} \beta \frac{h^2}{mR^2} = 80 A^{1/3} \text{ MeV},$$

 β = 24 MeV, nuclear radius $R = 1, 2A^{1/3} fm$; A is the nucleon count.

The next step [7] enables us to explain the splitting of the quadrupole deformation of the nuclei into two components. In non-spherical nuclei, which have the form of axially symmetric ellipsoids, there should be two resonant frequencies (i.e., dipole vibrations and dipole resonances should be split into two components), corresponding to movements along and across the symmetry axis of the nucleus. This leads to a broadening of the photoabsorption cross section and to the appearance of two photoabsorption maxima (see fig. 2) as a reaction of the nucleus to the photon flux [5, 6, 9].

It may be that the double peaks in the $\varepsilon(T)$ and $\sigma(T)$ dependences at the T_c for pure TGS crystals, PAA and PANa polymers, holmium and yttrium formates are related to the splitting of the maxima of these properties for the energy levels of non-spherical nuclei [7]. The main question is in which ranges these levels exist and how they can be detected. It is possible that for the OH...O network, transitions of protons and neutrons between levels lying above the ground level occur at frequencies of 10^{-2} – 10^4 Hz at temperatures from 4 to 450 K, and electronic transitions occur only at femto-range frequencies near 0 K.

Dielectric spectroscopy of crystalline hydrates, polymers, biopolymers and other materials with an *OH...O* network provides an extensive experimental basis for studying the effect of dipole interactions and for an analysis using the

principles of quantum physics. Fig. 3 illustrates the results of measuring low-frequency resonances $(10^{-1}-10^3 \, \text{Hz})$ corresponding to temperatures close to room temperatures, as well as to low temperature regions $4-200 \, \text{K}$. In fig. 4, the $\varepsilon(T)$, $\sigma(T)$, and j(T) dependences are shown for a number of polymers and crystals where the splitting is detectable; however, it persists in the range of 0,1-1,5 Hz. Broader areas of deviation from ε_{max} can be 5-15 K large (see TGS, DGN, TGTel, holmium formates, PAA, PANa) (see fig. 3, 4).

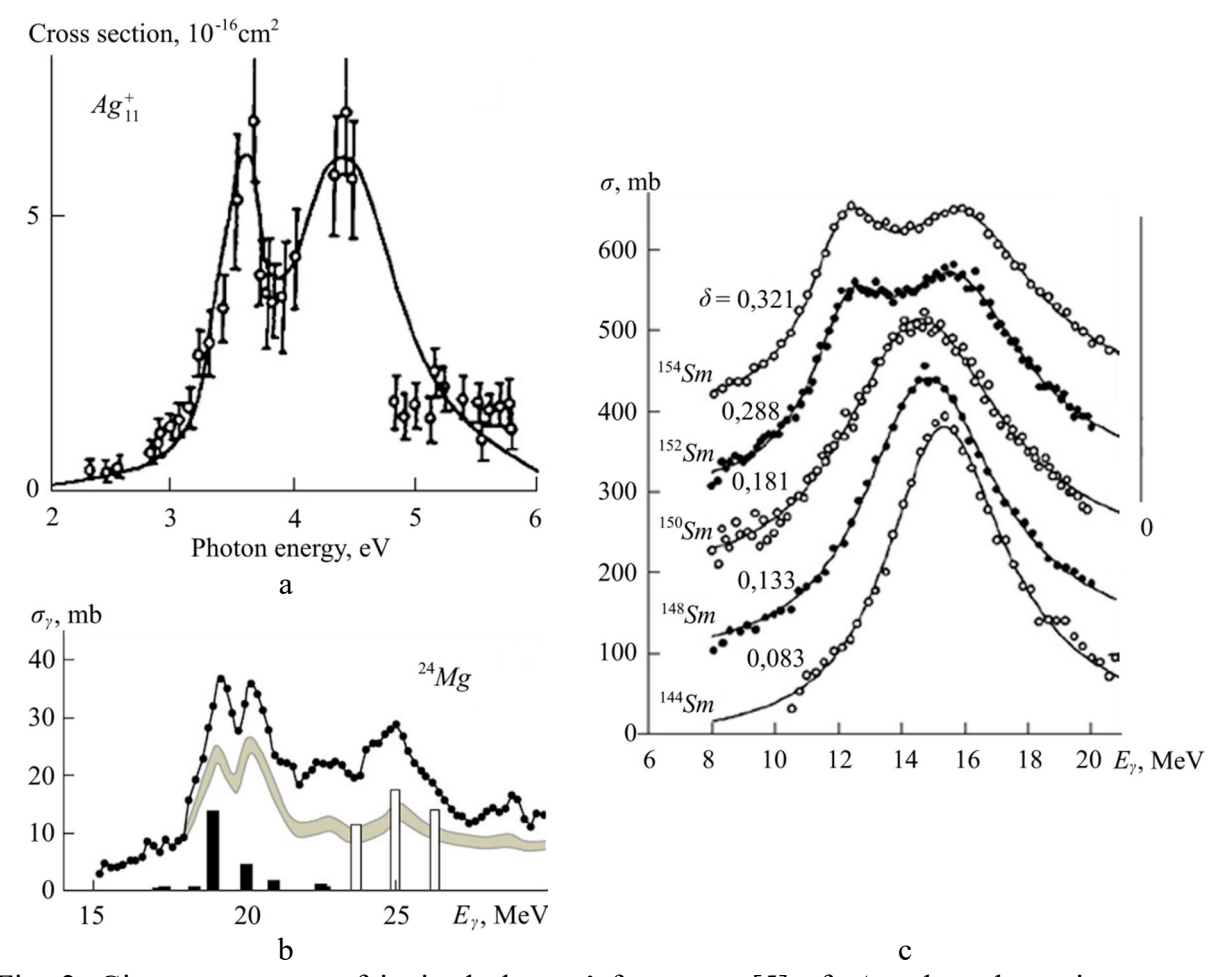


Fig. 2. Giant resonances of ionized clusters' fragments [5] of Ag photoabsorption cross-sections (a); photoabsorption cross-section for the 24 Mg nucleus obtained by the summation of photoproton and photoneutron absorption (b) [6]; photoneutron sections of Sm isotopes with their reduced quadrupole deformation parameters (c) [6, 7].

Previously, we associated this phenomenon with the transition from the excited level to the ground level causing the rearrangement of the entire *OH...O* network, but since the levels are close to each other and close to the upper level of the binuclear potential, tunnelling is possible. The splitting may result from the presence of ellipsoid nuclei with two symmetry axes.

Doubled maxima were also observed on the $\varepsilon(T)$ dependences (see fig. 4)

for triglycine tellurate in the regions below 49–93°C. But TGTel is a linear pyroelectric, not a ferroelectric, i.e., it does not have a ferroelectric transition. The structure of TGTel is isomorphic to the structure of TGS. It is possible that the reason behind that is the dipole deformation of O^{2-} nuclei.

Two maxima of $\sigma(T)$ and $\varepsilon(T)$ dependences in the range of $84\pm6^{\circ}$ C are observed for temperatures of ~89,5°C and 75°C only at frequencies of 10^{-1} Hz, 1,36 Hz, and 10,2 Hz. At higher frequencies, there is no splitting (within the measurement error). The measurements were carried out using the Novocontrol Concept 40 instrument in the frequency range of 10^{-2} – 10^{7} Hz for temperatures of $0-100^{\circ}$ C. The accuracy of temperature stabilisation was $0.1-0.3^{\circ}$ C.

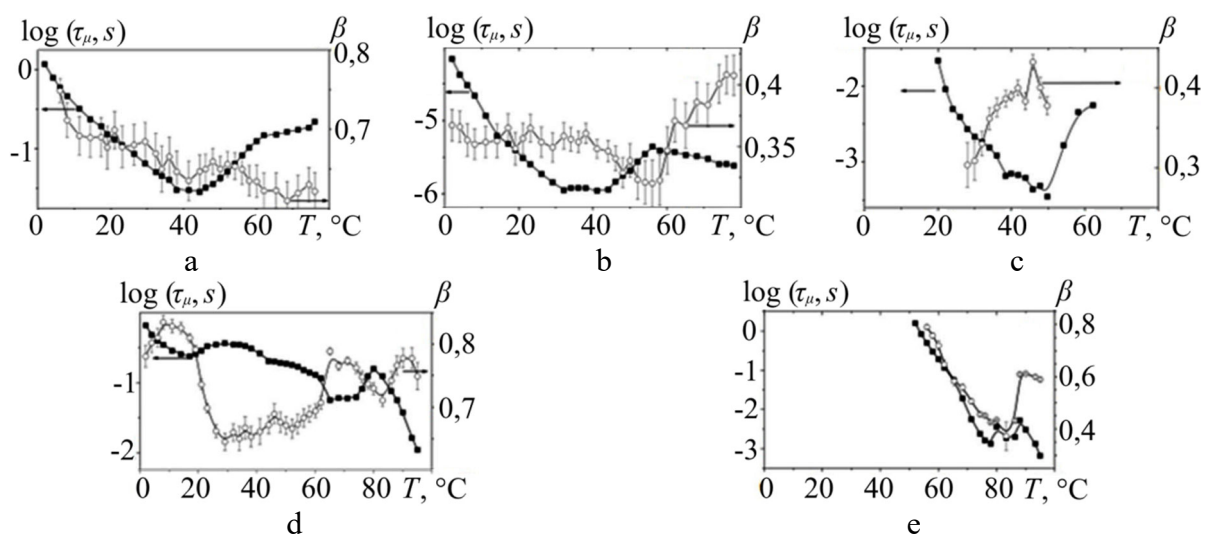


Fig. 3. Temperature dependences of the conductivity relaxation time, τ_{μ} (left), and of the β coefficient of the Kohlrausch-Witt function (right) for PAA (a), PANa (b), holmium formate (c), TGTel crystal (d) and DGN (e). The β coefficient reflects the deviation of the width of the τ_{μ} spectrum from the Debye function ($\beta = 1$) due to changes in the number of current carriers, their mobility, and in the number of clusters [10].

Finally, another mystery: a pure TGS crystal is a ferroelectric with a phase transition at T_c = 49,7°C. Below the T_c in the polar phase, crystal plates [010] immediately form multi-domain structures (see fig. 5) which have a maximum in T_c and obey the law $1/\varepsilon(T)$ above and below the T_c . ATGS crystals doped with chromium (less than 0,06 wt.%) and L-alanine (0,06 wt.%), at temperatures below T_c , grow as single-domain crystals, which are polarised at T > 140°C (see fig. 5 a, b).

Doping of TGS is done by the introduction, at the growth stage, of metallic impurities, such as chromium and copper, and by the substitution of glycine ion by L, α -alanine. In the $NH_3^+CH_2COOH$ ionic fragment of the TGS molecule, NH_3 group is replaced by an ion which is irreversible (relative to the

mirror plane of polarization). The substitution of the irreversible patterns can fix the position of the NH_3 group onto one of the sides of the mirror plane. The resulting internal field E_{dp} depends on the amount of L, α -alanine (0,01-0,04 wt.%) and chromium (0,06-0,1 wt.%) impurities. The maximum E_{dp} is 26-28 kV/cm.

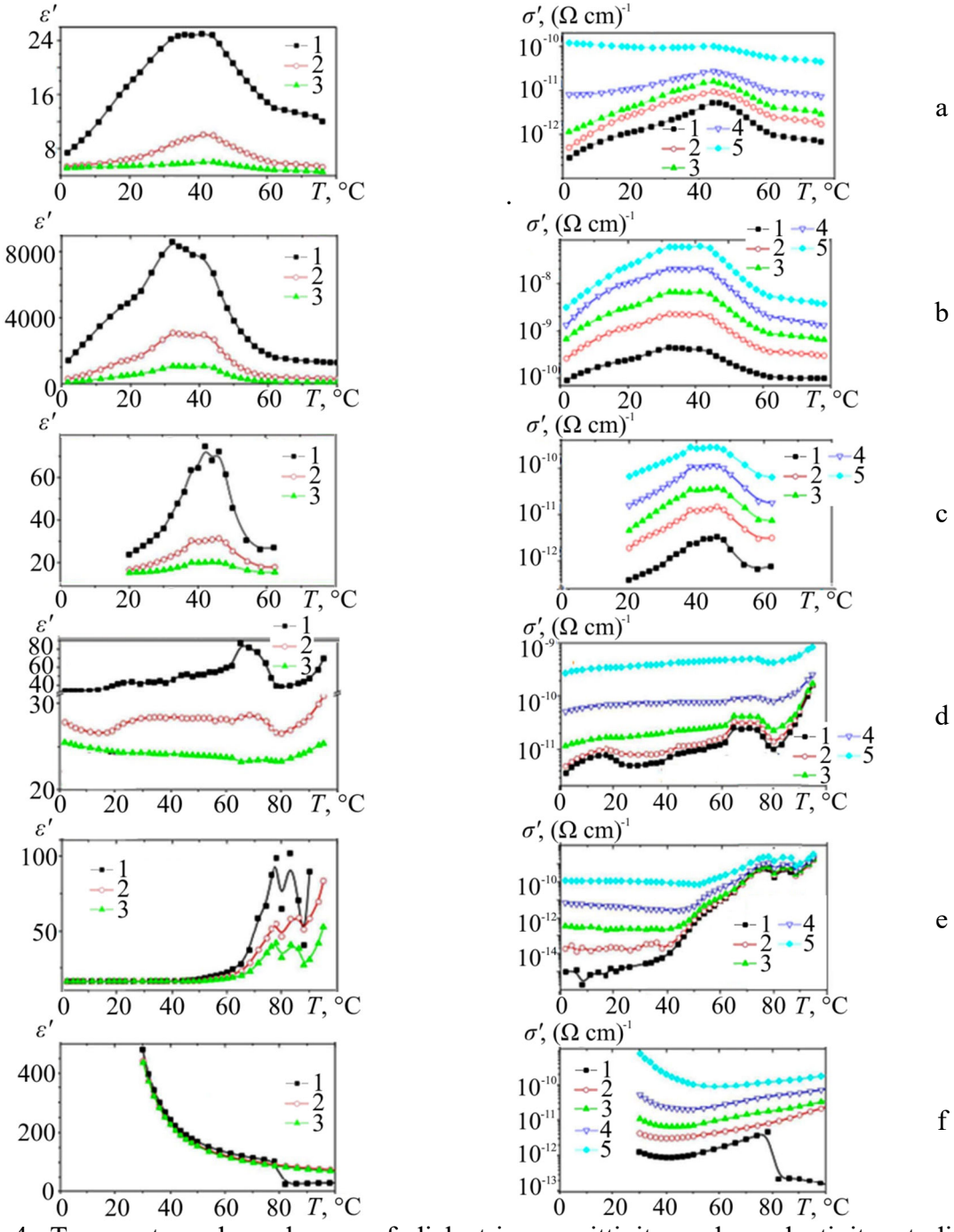


Fig. 4. Temperature dependences of dielectric permittivity and conductivity at different frequencies for polymers PAA (a), PANa (b), holmium formate (c) and crystals DGN (d), TGTel (e), TGSel (f). 1-0.1 Hz, 2-1.36 Hz, 3-10.2 Hz, 4-108 Hz, 5-1.13 kHz.

In terms of structure, ligand molecule should present a polar irreversible pattern or an ion with a maximum charge. The size of the substituted ligand should be close to that of the fragment of the TGS molecule which is to be substituted, whereas the size of insertion ligands (such as chromium or iron) should be close to the size of the interstitial lattice site.

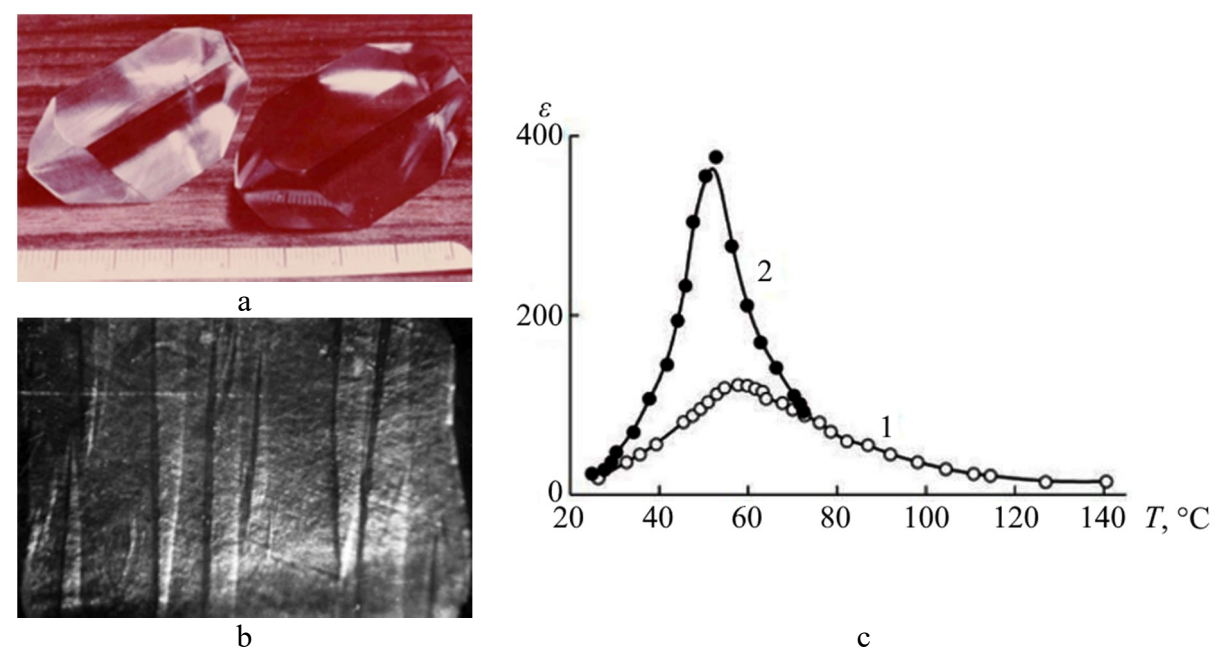


Fig. 5. Photographs of artificial crystals of TGS (a), TGS doped with alanine and chromium (a), the domain structure of pure TGS (b) and temperature dependence of the dielectric permittivity (c) of a TGS crystal doped with L, α -alanine (0,04 wt.%) and chromium (0,06 wt.%) (curve 1); doped with copper (0,01 wt.%) (curve 2).

In TGS, ligands are chelate complexes formed in a solution of TGS+ Cr^{3+} . For their growth, it is important that the quantum fields of any TGS and ATGS+ Cr^{3+} particles are coherent, so that they can receive information through the spin of photons and align themselves parallel to each other, according to the position of the $\langle + \rangle$ – $\langle - \rangle$ dipole.

When L, α -alanine and chromium or copper salts are added to the solution of TGS, chelate complexes are obtained. When a molecule of a chelate complex hits the ledge of a growing crystal, the molecule's P_s aligns itself parallel to E_{dp} , and the direction of the P_s coincides with that of E_{dp} . The coherence area of the chelate complex may be much larger than the analogous region of the TGS molecule, which results in the expansion of the domain width so that it becomes larger that the size of the growing surface. But even though the number of the molecules of chelate complexes is hundreds and thousands of times smaller than the number of TGS molecules in solution, the newly formed molecules of chelate complexes make the entire volume of the crystal a single domain. Crystals doped with alanine and chromium (about 0,05 wt.% and

0,06 wt.%, respectively) have found application in pyrocon and pyrovision devices, temperature sensors, etc. Thus, coherence and correlation are quantum features that manifest themselves in single-domain chromium-doped ATGS crystals.

Impurity point defects, even in insignificant concentrations, give rise to vibrations that do not exist in an ideal crystal, and change the thermodynamic and kinetic characteristics of crystals. The most significant for the polar properties of lattice are vibrations caused by defects whose frequencies lie in the range of the allowed energies of the vibrational spectrum of the ideal base crystal. These vibrations are termed quasi-local. Quasi-local vibrations are characterized by large amplitude of oscillations of the impurity ion itself or of those atoms with which it interacts directly (an impurity cluster). Quasi-local vibrations are a package of normal modes and, accordingly, have a continuous spectrum of finite width in the zone of excited vibrations.

During the growth of the pure TGS crystal from an aqueous solution, polar «stripes» grow on the growth ledges of the perfectly smooth seed (no domain boundaries are observed on the chip of the polar section of the crystal), in each of which the P_s vector is oriented in the direction of the axis $\overline{2}$ of the TGS crystal (see fig. 5 c). Since the growing crystal is in an aqueous solution of glycine molecules, a single-domain stripe is formed after some time (several minutes), with the direction of the dipole (i.e., of the spins) such that the positive charge is oriented towards the upper side. But coherence does not eliminate the accumulation of the electric field E_{dp} between the two surfaces of the domain, and therefore a new second domain with antiparallel dipoles (spins) is produced. This reduces the E_{dp} field on the surfaces of the two domains, and when it approaches zero, a new domain is generated whose spins are aligned with the first domain. The width of all domains for TGS growing at temperatures below 49° C (T_c) is 0,01 mm, and the internal field E_{dp} is on the order of tens of kV/cm and ~ 28 kV/cm for chromium-doped ATGS.

The layered growth of a crystal from an aqueous solution occurs due to the movement of the ledges. Impurities reduce the growth rate: in the presence of an Fe^{3+} admixture in an amount of $10^{-60}\%$, the growth rate of the HF crystal is reduced by an order of magnitude. The height of the growing crystal face edge depends on the height of the growth ledge.

In the first works on the construction of lasers, a ruby crystal (corundum Al_2O_3 doped with chromium ions, 0,05 wt.%) was used. This system was called a three-level quantum photon generator. Figure 6 shows the operation scheme: three energy levels of the Cr^{3+} ion are used. The ground state corresponds to the E_1 level, the excited state corresponds to the E_2 levels (the number of levels is very large, and the lifetime at an E_2 level of chromium is about 10^{-8} s), and E_3 is

an excitation level between E_2 and E_1 . The accumulation of chromium ions at the E_3 level occurs due to the fact that the lifetime of the chromium ion at the E_3 level is 10^{-3} s, which is significantly larger than that at the higher energy level E_2 (10^{-8} s). The stimulated transition from E_3 to E_1 is resonant. A photon that stimulates the E_1 -to- E_2 transition generates a photon of the same frequency v, which is transmitted to another chromium ion; this stimulates a new transition, i.e., the first photon generates two photons.

The monochromatic wave of coherent light has a wavelength of 693 nm, which corresponds to the red region of the electromagnetic spectrum, so the colours of ruby and of the ATGS+ Cr^{3+} (chromium content of 0,05-0,06 wt.%) crystal are close to dark red (see fig. 5 a, b). All photons born in the transition from the E_3 to E_1 level have same frequencies and spin directions.

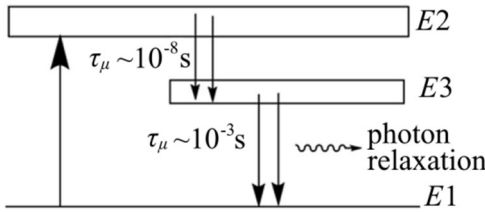


Fig. 6. Diagram of the energy levels of the two-minima potential of chromium-doped (0,06 wt.%) ruby and of TGS doped with chromium (0,06 wt.%) and alanine (0,04 wt.%). Inset: photon flux model.

A similar scheme of inverse level population also exists in other substances, possibly in crystals of L, α -TGS+ Cr^{3+} as well. Since in our crystal, as in ruby, there is an admixture of chromium in the same amount of 0,06 wt.%, then with the growth of the ATGS+ Cr^{3+} crystal in the ferroelectric phase, an uncompensated electric displacement field E_{dp} may arise, which will contribute to the throwing of Cr^{3+} ions onto the E_2 level (from the zone of excited levels). A non-radiative transition $E_2 \rightarrow E_3$ (from the upper level to the lower level E_3) occurs spontaneously or under the action of a photon – in a collision with other particles in solution or with photons, its energy is spent on heating the crystal and solution.

The ions accumulated at the E_3 level pass to the E_1 level, giving birth to photons – to the powerful monochromatic coherent laser radiation. In a laser, the radiation is narrowly directed thanks to mirrors at the ends of the ruby rod. In the case of monodomenisation at the stage of growth of triglycine sulphate crystals doped with alanine and chromium, this coherent radiation spreads over a greater distance and the dipoles of the growth seeds line up in the same direction along the field. This phenomenon is a kind of dipole resonance and polarization-entangled photons.

Thus, the formation of a single-domain uniformly-coloured ATGS+ Cr^{3+} crystal as a consequence of a coherent dipole action of an electromagnetic field or a photon flux on chromium nuclei at large distances is an indirect manifestation of the giant dipole resonance and it's quantum nature.

The «plateau» in the $\varepsilon(T)$ dependence for a ferroelectric crystal under stage heating could be explained as follows: the emerging electric displacement fields E_{dp} contribute to the population of levels which are close to the zone of excited levels near the maximum energy level. However, in the case of LTT, KDP crystals and a number of its isomorphs (CsDP, RDP) (see fig. 7) this also could happen for levels neighbouring E_2 [11, 19]. The proximity of the levels, which are populated by ions or protons of hydrogen bonds, leads to vigorous tunneling in a wide temperature range: from ~4 to 13 K for LTT, from ~100 to 123 K (T_c) for KDP. In isomorphs of KDP, tunnelling occurs in the range from (T_c – 20 K) up to the T_c of the corresponding crystal [11, 19].

The available observations of the rapid growth of the ledges show their relative stability (at low supersaturations) and the constancy of the movement rate (the ledge height is 0,1 mm).

In our experiments on the growth of ATGS+ Cr^{3+} from an aqueous solution at a temperature of 30-40°C, the procedure begins with the preparation of a solution of triglycine sulphate, L, α -alanine, and a chromium salt in quantities sufficient to obtain the desired supersaturation and seed on which the stepwise growth will begin. Usually it is a single-domain plate, a polar section of a very pure TGS monocrystal of a given size. A characteristic feature of the TGS growth in the polar phase (below T_c = 49,7°C) is that the «embryos» occupying a trihedral angle already have a dipole moment and are deployed so that the P_s of an embryo coincides with the P_s of spontaneous polarisation of the growing crystal. It is obvious that for growth in the quantum field which is formed in the volume of the solution, the orientation of the building blocks of the crystal is sufficient.

The unusually high proton mobility along the H-Bond network of clusters exceeds the mobility of Na and K alkaline ions. The correlated proton mobility over a short distance plays an important role in the formation of the total charge and dipole moment when an electric field is applied. In the vicinity of the "threshold" temperature points an increase in the number of active protons contributes to an increase in the dielectric constant and conductivity.

A large group of results is TSDC experimental data obtained in the stepwise heating mode in the range from 20 to more than 100°C for semicrystalline (VDF/TrFE copolymer) and crystalline (TGS) materials (see fig. 8) [12, 13, 15]. TGS crystals (pure and doped) have a network of *OH...O* H-Bonds like in water. Hopping charge transfer along the network, and, possibly,

tunneling, contributes to the value of the current. Experiments show that impurities order the TGS crystal structure (monodomainization), which leads to an increase of TSDC by 1-2 orders of magnitude. TSDC peak in pure and doped TGS are observed near «threshold» temperature point and TSDC passes through zero at 60-65°C.

Different materials absorb water vapor differently. For example, in SiO_2 part of water is bound: water molecules are fixed in cracks as well as on the surface and in semiclosed voids (cavities) [7]. Part of the molecules cannot be removed by drying even in vacuum [16]. Similar processes can occur at the preparation of polymer films. For example, the preparation method of the hydrophobic PVDF/TrFE polymer films includes annealing at temperatures above 100°C followed by sharp cooling in water, so water molecules enter the surface layer and bind to polymer molecules. TSDC curve for VDF/TrFE passes through zero near 50°C, where the hydrogen level of the proton in the double-well potential is overpopulated. The first maximum for VDF/TrFE, similar to that for TGS, is observed at 30-40°C. The j(T) minimum is observed in the region of 75°C, as well as additional maximum near 110°C. The temperatures of 49,7 and 110°C are the temperatures of phase transitions for TGS and PVDF/TrFE, respectively.

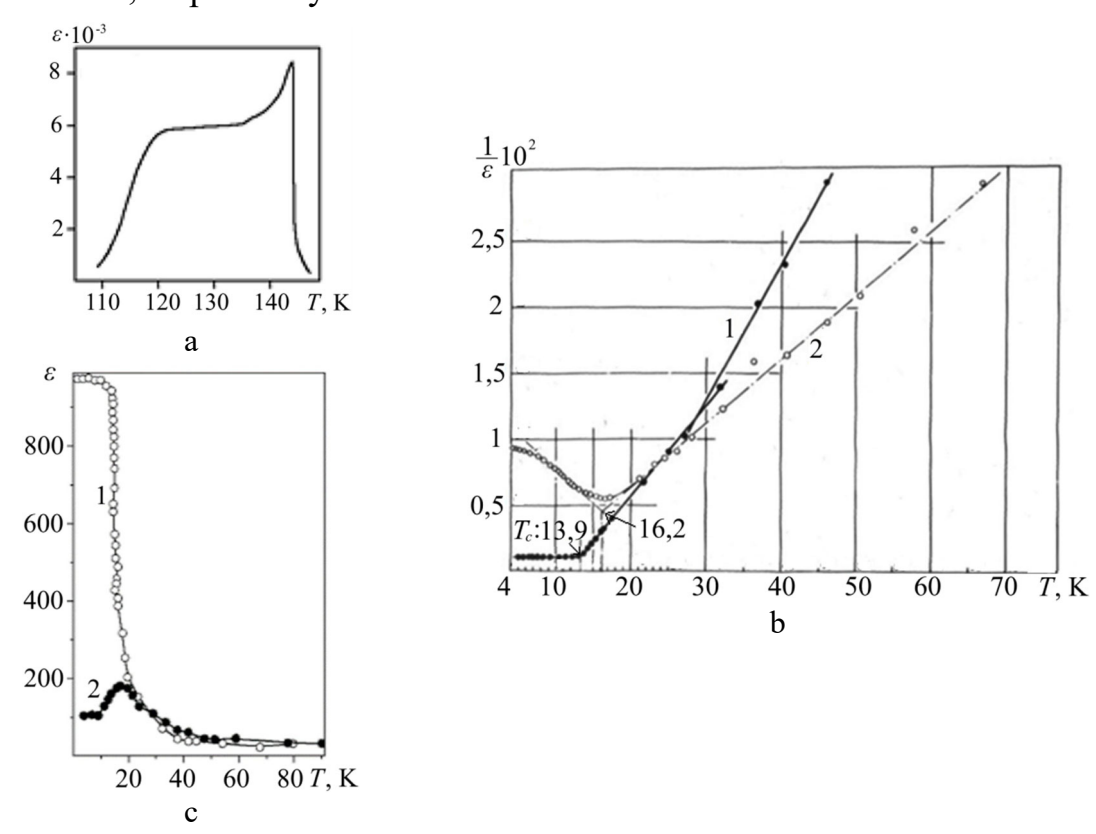


Fig. 7. Temperature dependences of the dielectric permittivity ε of RbH_2PO_4 (RDP) (a) and lithium-thallium tartrate (LTT) (b, c) monocrystal near the respective Curie points T_c . Curves 1 - E = 0; 2 - E = 4 kV/cm.

In a number of papers devoted to the TSDC studies of organic materials, the role of the currents in life processes of biological systems is noted (see, for example, [20]). Comparison of the TSDC spectra of fine-grained mica and venous human blood showed that the currents are due to the presence of water with different degrees of structuring. If we pay attention to the temperatures of j(T) anomalies of these materials, then for the mica there are maxima in the regions of 35 and 64°C; for venous blood – at 30, 60 and 80°C, and a transition through zero around 90°C [21].

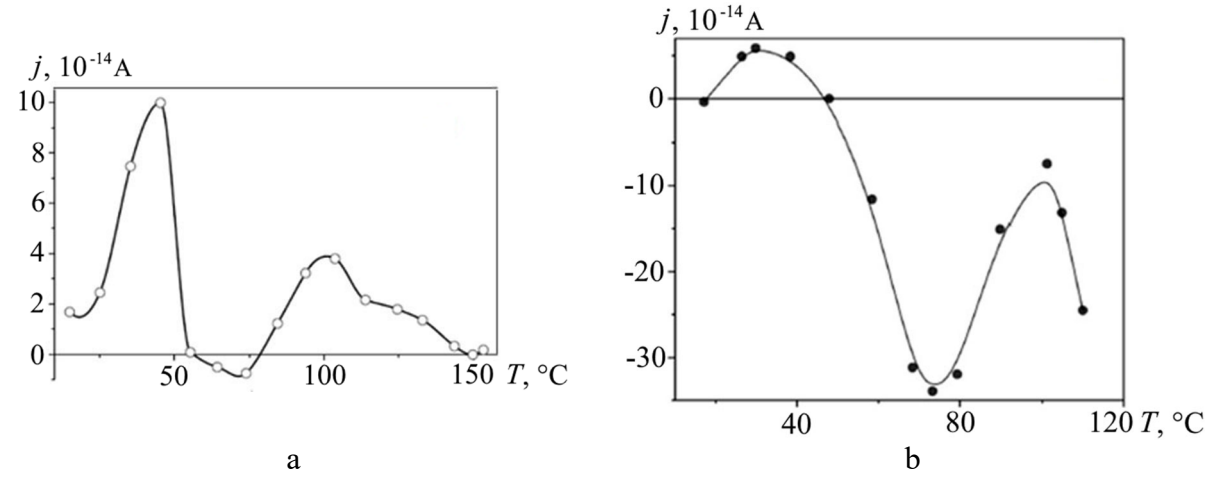


Fig. 8. TSDC curves obtained during the stepwise heating of TGS (a) and PVDF/TrFE 70/30 semicrystalline polymer (b).

We can suppose that, simultaneously with the rearrangement of the network of water or OH...O bonds with dO-O 2,7-2,8 Å, the entire system is rearranged. In crystals of the TGS group, the temperatures of phase transitions are close to the «threshold» points of water: 20°C for triglycine selenate, 49,7°C for TGS and 85°C for triglycine fluoroberyllate. It is possible that H-Bonds act as «triggers» of the ferroelectric phase transition. This point of view arose already in the 1970s for crystals of potassium dihydrogen phosphate (Slatter's model) [22] and TGS [23]. Correlated proton displacements in the network of OH...O bonds in electric field is confirmed by NMR and PMR spectroscopy data.

Numerous papers on computer modeling of physical and chemical processes (IR spectra, NMR, etc.) in materials containing networks of OH...O, NH...O, CH...N, etc. hydrogen bonds, have shown that the temperature change in the molecular dynamics model depends on the addition of the nuclear quantum effect (NQE) to the classical mechanism.

The manifestations of this effect are [12, 23, 24]:

- In IR and NMR spectra at low temperatures and high frequencies, an asymmetry is observed in the curves of the wave functions of the system;

- The temperature T_c of the order-disorder transition changes when H is replaced by D. Even with a D content is of the order of several percent, T_c shifts by tens of degrees [25];
- Tunneling prevails when the proton energy approaches the level of the barrier energy of the double-well potential (especially in the temperature range of liquid helium) [19, 23, 24].

Dielectric ordering of water molecules present in the dipole lattice was experimentally observed near absolute zero temperatures as a ferroelectric phase transition at 13K [19] in lithium-thallium tartrate monohydrate, as well as in aqueous cordierite crystals $(Mg, Fe)_2 Al_4 Si_5 O_{18}$ [23]. No ferroelectric properties were found in anhydrous cordierite.

In order to calculate the energy levels and wave functions, the Schroedinger equation was numerically integrated [24]. To follow the dynamics of the system with temperature or internal and external fields, it is necessary to have data on the energies of states in the total potential and individual half potentials, as well as the corresponding overlap integrals and the matrix elements of the half potentials.

Numerical estimates of the energy levels corresponding to the motions of bridge protons in molecular rings of $(H_2O)n$ clusters, in case of symmetric potential (n=4, 6, 8 and 12) are equal in the left and right half-potentials. Accordingly, in the «full» potential in the energy range from the minimum of the potential up to two-thirds of the barrier height, all states are doubly degenerate (accurate to 10^{-1} cm) and noticeably interact at higher energies, which leads to the splitting of excited energy levels. When the position of the potential walls changes, the number of levels in the potential wells and their energies change. In large clusters representing cell-type structures, the combined vibration can have a frequency even lower than the contraction/expansion frequencies of the structure. The motions of bridge protons are strongly associated with the motions of clusters in which the bridge protons oscillate, or with swinging of free OH-groups [24].

The behaviour of $\varepsilon(T)$, $\sigma(T)$, and $\tau_{\mu}(T)$ around the «threshold» points can be compared with a long-term collective resonance. This is the strongest reaction of atomic nuclei to electromagnetic radiation, being the fundamental universal collective excitation of nuclei, inherent to all nuclei.

In resonance, all protons synchronously and coherently oscillate relative to all neutrons with a frequency of $\sim 10^{-22}$ Hz, forming a dipole of nuclear dimensions ($\sim 10^{-12}$ cm). This nuclear process can be caused by the absorption of a γ -quantum with high energy or by the internal electric displacement field E_{dp} of a polar dielectric, emerging due to a stepwise temperature change: E_{dp} can reach tens and hundreds of kilovolts.

4. Conclusions

In this study, we investigated the dielectric properties (ε , σ) of polymers and crystals containing water or OH...O bonds at temperatures T from -40 to 140°C and from 4 to 20 K for LTT. Since water and OH...O networks form clusters during stage heating, the cluster structure is rearranged at certain temperature points, termed «threshold» points. In the vicinity of these points, dielectric ($\varepsilon(T)$, $\sigma(T)$) and other characteristics increase several times, and for frequencies from 0,07 Hz to 1000 Hz – by an order of magnitude or more. This phenomenon can be compared with giant dipole resonance. In order to explain the maxima of ε , σ , etc. at threshold points, we propose using the concept of GDR, which is a quantum cooperative coherent excitation of nuclei involving all protons and neutrons of nucleus, caused by electric dipole photons E_1 . For an energy core (an axially symmetric ellipsoid), the same model makes it possible to explain the splitting of a parameter's peak (for atomic nuclei, metal clusters and fullerenes).

We observed this phenomenon for $\varepsilon(T)$, $\sigma(T)$, and $\tau_{\mu}(T)$ in PAA, PANa polymers, holmium formates, PVDF-TrFE and crystals of TGTel and DGN. Furthermore, for the single-domain growth of alanine- and chromium-doped TGS, we observed a «plateau» before the Curie point of the $\varepsilon(T)$ dependence in KDP and LTT crystals. It is possible that ion or proton tunneling occurs due to a large number of energy levels in the double-well potential in the zone of excited E_2 levels.

References:

- 1. Chaplin M.F. *Structure and properties of water in its various states*, Encyclopedia of Water: Science, Technology, and Society; ed. by P.A. Maurice, 2019, 19 p. DOI: 10.1002/9781119300762.wsts0002.
- 2. Drechsel-Grau C., Marx D. Protons in concert. *Nature Physics*, 2015, vol. 11, issue 3, pp. 216-218. DOI: 10.1038/nphys3269.
- 3. Cantrell W., Ewing G.E. Thin film water on muscovite mica. *The Journal of Physical Chemistry B*, 2001, vol. 105, issue 23, pp. 5434-5439. DOI: 10.1021/jp004305b.
- 4. Gavrilova N.D., Malyshkina I.A., Novik O.D. Thermally stimulated depolarization currents in TGS crystals with impurities and radiation defects under stepwise heating, *Moscow University Physics Bulletin*, 2020, vol. 75, issue 3, pp. 242-248. DOI: 10.3103/S0027134920030091.
- 5. Tiggesbäumker J., Köller L., Meiwes-Broer K.-H. Bound-free collective electron excitations in negatively charged silver clusters, Chemical Physics Letters, 1996, vol. 260, issue 3-4, pp. 428-432. DOI: 10.1016/0009-2614(96)00950-5.
- 6. Varlamov V.V., Ishkhanov B.S., Kapitonov I.M. et al. On the role of nucleons of different shells in the formation of the giant dipole resonance of the 24Mg nucleus, *Soviet Journal of Nuclear Physics*, 1979, vol. 30, no. 5, pp. 617-622.
- 7. Ishkhanov B.S., Kapitonov I.M. Giant dipole resonance of atomic nuclei. Prediction, discovery, and research. *Physics-Uspekhi*, 2021, vol. 64, issue 2, pp. 141-156. DOI: 10.3367/UFNe.2020.02.038725.
- 8. Migdal A. Quadrupole and dipole γ -radiation of nuclei, *Journal of Physics Academy of Sciences of the USSR*, 1944, vol. 8, issue 1-6, pp. 331-336.
- 9. Carlos P. The giant dipole resonance in the transition region of the samarium isotopes, *Nuclear Physics A*, 1974, vol. 225, issue 1, pp. 171-188. DOI: 10.1016/0375-9474(74)90373-X.
- 10. Jonscher A.K. Dielectric relaxation in solids, *Journal of Physics D: Applied Physics*, 1999, vol. 32, issue 14, pp. R57-R70. DOI: 10.1088/0022-3727/32/14/201.

Физико-химические аспекты изучения кластеров, наноструктур и наноматериалов. — 2024. — Вып. 16

- 11. Novik O.D., Malyshkina I.A., Gavrilova N.D. Dielectric ordering of water molecules in the dipole lattice of potassium hexacyanoferrate (II) trihydrate. *Ferroelectrics*, 2022, vol. 600, issue 1, pp. 124-136. DOI: 10.1080/00150193.2022.2115804.
- 12. Gavrilova N.D., Novik V.K., Malyshkina I.A. The role of water in the anomalies of pyro- and thermodepolarization properties of pyroactive polymer films at stepwise heating, *Journal of Non-Crystalline Solids*, 2018, vol. 483, pp. 60-64. DOI: 10.1016/j.inoncrysol.2017.12.056.
- 13. Gavrilova N.D., Novik V.K. On the role of a weak hydrogen bond OH...O in the formation of the anomalous dielectric response of crystals and polymers near 40°C, *Moscow University Physics Bulletin*, 2011, vol. 66, issue 3, pp. 260-266. DOI: 10.3103/S0027134911030076.
- 14. Gavrilova N.D., Malyshkina I.A., Makhaeva E.E. et al. Dielectric relaxation anomalies in polyacrylic acid and their relationship with «critical» points of water, *Ferroelectrics*, 2016, vol. 504, issue 1, pp. 3-14. DOI: 10.1080/00150193.2016.1238284.
- 15. Gavrilova N.D., Malyshkina I.A., Novik O.D. A special role of water in dielectrics of different structural organization, *Ferroelectrics*, 2021, vol. 585, issue 1, pp. 40-51. DOI: 10.1080/00150193.2021.1991219.
- 16. Gavrilova N.D., Malyshkina I.A. The influence of changes in the structure of hydrogen bonds of water on the electrophysical properties of matrix—water systems in stepwise heating, *Moscow University Physics Bulletin*, 2018, vol. 73, issue 6, pp. 651-658. DOI: 10.3103/S0027134918060127.
- 17. Verkhovskaya K.A., Gavrilova N.D., Novik V.K. et al. Low-frequency dielectric dispersion and pyroelectric effect inferroelectric vinylidene fluoride trifluoroethylene copolymer in phase transitions, *Moscow University Physics Bulletin*, 1997, vol. 52, issue 3, pp. 55-66.
- 18. Gavrilova N.D., Makhaeva E.E., Malyshkina I.A., Khokhlov A.R. Dielectric response of polyampholytes with different structures, *Polymer Science, Series B*, 2018, vol. 24, issue 11-12, pp. 379-383.
- 19. Gavrilova N.D., Malyshkina I.A., Novik O.D. Hydrogen bond as a trigger of ferroelectric-like phase transition in lithium-thallium tartrate monohydrate. *Ferroelectrics*, 2021, vol. 582, issue 1, pp. 1-11. DOI: 10.1080/00150193.2021.1951029.
- 20. Gaur M.S. Thermally stimulated current analysis in human blood, *Trends in Biomaterials and Artificial Organs*, 2007, vol. 21, issue 1, pp. 8-13.
- 21. Shcherbachenko L.A., Borisov V.S., Maksimova N.T. et al. Electret effect and electrotransport in disperse organic and inorganic systems, *Technical Physics*. 2009, vol. 54, issue 9, pp. 1372-1379. DOI: 10.1134/S1063784209090199.
- 22. Slater J. Theory of the transition in KH₂PO₄, *The Journal of Chemical Physics*, 1941, vol. 9, issue 1, pp. 16-33. DOI: 10.1063/1.1750821.
- 23. Belyanchikov M.A., Savinov M., Bedran Z.V. et al. Dielectric ordering of water molecules arranged in a dipolar lattice, *Nature Communications*, 2020, vol. 11, issue 1, art. no. 3927, 9 p. DOI: 10.1038/s41467-020-17832-y.
- 24. Bednyakov A.S., Novakovskaya Y.V. Formation of charged H₃O⁺ and OH⁻ fragments at consistent shifts of protons in water clusters. *Russian Journal of Physical Chemistry A*, 2016, vol. 90, issue 9, pp. 1813-1821. DOI: 10.1134/s0036024416090041.
- 25. Zhukov S.G., Kulbachinskii V.A., Smirnov P.S. et al. Vliyanie gidrostaticheskogo davleniya na fazovye perekhody v kristallakh $K(H_{(1-x)}D_x)_2PO_4$ [Influence of the hydrostatic-pressure on phase-transitions in $K(H_{(1-x)}D_x)_2PO_4$ crystals], Izvestiya Akademii nauk SSSR Seriya fizicheskaya [Bulletin of the Academy of Sciences of the USSR. Physical Series], 1985, vol. 49, no. 2, pp. 255-258. (In Russian).

Библиографический список:

- 1. **Chaplin, M.F.** Structure and properties of water in its various states / M.F. Chaplin // In: Encyclopedia of Water: Science, Technology, and Society; ed. by P.A. Maurice. 2019. 19 p. DOI: 10.1002/9781119300762.wsts0002.
- 2. **Drechsel-Grau, C.** Protons in concert / C. Drechsel-Grau, D. Marx // Nature Physics. 2015. V. 11. I. 3. P. 216-218. DOI: 10.1038/nphys3269.
- 3. **Cantrell, W.** Thin film water on muscovite mica / W. Cantrell, G.E. Ewing // The Journal of Physical Chemistry B. 2001. V. 105. I. 23. P. 5434-5439. DOI:10.1021/jp004305b.
- 4. **Gavrilova, N.D.** Thermally stimulated depolarization currents in TGS crystals with impurities and radiation defects under stepwise heating / N.D. Gavrilova, I.A. Malyshkina, O.D. Novik // Moscow University Physics Bulletin. 2020. V. 75. I. 3. P. 242-248. DOI: 10.3103/S0027134920030091.
- 5. **Tiggesbäumker, J.** Bound-free collective electron excitations in negatively charged silver clusters / J. Tiggesbäumker, L. Köller, K.-H. Meiwes-Broer // Chemical Physics Letters. 1996. V. 260. I. 3-4. P. 428-432. DOI: 10.1016/0009-2614(96)00950-5.

Физико-химические аспекты изучения кластеров, наноструктур и наноматериалов. — 2024. — Вып. 16

- 6. **Varlamov**, **V.V.** On the role of nucleons of different shells in the formation of the giant dipole resonance of the 24Mg nucleus / V.V. Varlamov, I.M. Ishkhanov, I.M. Kapitonov et al. // Soviet Journal of Nuclear Physics. −1979. − V. 30. − № 5. − P. 617-622.
- 7. **Ishkhanov, B.S.** Giant dipole resonance of atomic nuclei. Prediction, discovery, and research / B.S. Ishkhanov, I.M. Kapitonov // Physics-Uspekhi. 2021. V. 64. I. 2. P. 141-156. DOI: 10.3367/UFNe.2020.02.038725.
- 8. **Migdal, A.** Quadrupole and dipole γ-radiation of nuclei / A. Migdal // Journal of Physics Academy of Sciences of the USSR. 1944. V. 8. I. 1-6. P. 331-336.
- 9. Carlos, P. The giant dipole resonance in the transition region of the samarium isotopes / P. Carlos // Nuclear Physics A. -1974. -V. 225. -I. 1. -P. 171-188. DOI: 10.1016/0375-9474(74)90373-X.
- 10. **Jonscher**, **A.K.** Dielectric relaxation in solids / A.K. Jonscher // Journal of Physics D: Applied Physics. 1999. V. 32. I. 14. P. R57-R70. DOI: 10.1088/0022-3727/32/14/201.
- 11. **Novik, O.D.** Dielectric ordering of water molecules in the dipole lattice of potassium hexacyanoferrate (II) trihydrate / O.D. Novik, I.A. Malyshkina, N.D. Gavrilova // Ferroelectrics. 2022. V. 600. I. 1. P. 124-136. DOI: 10.1080/00150193.2022.2115804.
- 12. **Gavrilova, N.D.** The role of water in the anomalies of pyro- and thermodepolarization properties of pyroactive polymer films at stepwise heating / N.D. Gavrilova, V.K. Novik, I.A. Malyshkina // Journal of Non-Crystalline Solids. 2018. V. 483. P. 60-64. DOI: 10.1016/j.jnoncrysol.2017.12.056.
- 13. **Gavrilova, N.D.** On the role of a weak hydrogen bond OH...O in the formation of the anomalous dielectric response of crystals and polymers near 40° C / N.D. Gavrilova, V.K. Novik // Moscow University Physics Bulletin. -2011.-V.66.-I.3.-P.260-266. DOI: 10.3103/S0027134911030076.
- 14. **Gavrilova, N.D.** Dielectric relaxation anomalies in polyacrylic acid and their relationship with «critical» points of water / N.D. Gavrilova, I.A. Malyshkina, E.E. Makhaeva et al. // Ferroelectrics. 2016. V. 504. I. 1. P. 3-14. DOI: 10.1080/00150193.2016.1238284.
- 15. **Gavrilova, N.D.** A special role of water in dielectrics of different structural organization / N.D. Gavrilova, I.A. Malyshkina, O.D. Novik // Ferroelectrics. 2021. V. 585. I. 1. P. 40-51. DOI: 10.1080/00150193.2021.1991219.
- 16. **Gavrilova**, **N.D.** The influence of changes in the structure of hydrogen bonds of water on the electrophysical properties of matrix—water systems in stepwise heating / N.D. Gavrilova, I.A. Malyshkina // Moscow University Physics Bulletin. 2018. V. 73. I. 6. P. 651-658. DOI: 10.3103/S0027134918060127.
- 17. **Verkhovskaya, K.A**. Low-frequency dielectric dispersion and pyroelectric effect inferroelectric vinylidene fluoride trifluoroethylene copolymer in phase transitions / K.A. Verkhovskaya, N.D. Gavrilova, V.K. Novik et al. // Moscow University Physics Bulletin. 1997. V. 52. I. 3. P. 55-66.
- 18. **Gavrilova**, **N.D.** Dielectric response of polyampholytes with different structures / N.D. Gavrilova, E.E. Makhaeva, I.A. Malyshkina, A.R. Khokhlov // Polymer Science, Series B. 2018. V. 24. I. 11-12. P. 379-383.
- 19. **Gavrilova, N.D.** Hydrogen bond as a trigger of ferroelectric-like phase transition in lithium-thallium tartrate monohydrate / N.D. Gavrilova, I.A. Malyshkina, O.D. Novik // Ferroelectrics. 2021. V. 582. I. 1. P. 1-11. DOI: 10.1080/00150193.2021.1951029.
- 20. **Gaur**, **M.S.** Thermally stimulated current analysis in human blood / M.S. Gaur // Trends in Biomaterials and Artificial Organs. 2007. V. 21. I. 1. P. 8-13.
- 21. **Shcherbachenko, L.A.** Electret effect and electrotransport in disperse organic and inorganic systems/L.A. Shcherbachenko, V.S. Borisov, N.T. Maksimova et al. // Technical Physics. 2009. V. 54. I. 9. P. 1372-1379. DOI: 10.1134/S1063784209090199.
- 22. **Slater**, **J.** Theory of the transition in KH_2PO_4 / J. Slater // The Journal of Chemical Physics. -1941. V. 9. -I. 1. -P. 16-33. DOI: 10.1063/1.1750821.
- 23. **Belyanchikov, M.A.** Dielectric ordering of water molecules arranged in a dipolar lattice / M.A. Belyanchikov, M. Savinov, Z.V. Bedran et al. // Nature Communications. 2020. V. 11. I. 1. Art. № 3927. 9 p. DOI: 10.1038/s41467-020-17832-y.
- 24. **Bednyakov**, **A.S.** Formation of charged H₃O⁺ and OH⁻ fragments at consistent shifts of protons in water clusters / A.S. Bednyakov, Y.V. Novakovskaya // Russian Journal of Physical Chemistry A. 2016. V. 90. I. 9. P. 1813-1821. DOI: 10.1134/s0036024416090041.
- 25. **Жуков**, С.Г. Влияние гидростатического давления на фазовые переходы в кристаллах К $(H_{1-x}D_x)_2PO_4$ / С.Г. Жуков, В.А. Кульбачинский, П.С. Смирнов и др. // Известия Академии наук СССР. Серия физическая. − 1985. − Т. 49. − № 2. − С. 255-258.

Физико-химические аспекты изучения кластеров, наноструктур и наноматериалов. — 2024. — Вып. 16

Оригинальная статья

Низкочастотная импедансная спектроскопия полимеров и кристаллов с сеткой водородных связей. Квантовые коллективные возбуждения ядер в молекулах

О.Д. Новик¹, Н.Д. Гаврилова¹, О.В. Малышкина²

ФГБОУ ВО «Московский государственный университет имени М.В.Ломоносова»
 119991, Россия, Москва, Ленинские горы, 1
 ²ФГБОУ ВО «Тверской государственный университет»
 170100, Россия, Тверская область, Тверь, ул. Желябова, 33

DOI: 10.26456/pcascnn/2024.16.239

Аннотация: В работе представлены результаты исследований температурно-частотного поведения диэлектрической проницаемости ε , проводимости σ , времени релаксации τ_{μ} , токов термодеполяризации j и пиротока γ в гидрофильных полимерах и кристаллах с сеткой водородных связей OH...O в диапазонах $0,01-10^7$ Гц и $20-140^{\circ}$ С. Анализ полученных данных выявил температурные аномалии $\varepsilon(T)$, $\sigma(T)$, $\tau_{\mu}(T)$, j(T), и $\gamma(T)$ вблизи «пороговых» точек 20, 36, 50, 65 и 85°С, где происходит разрушение кластеров воды (а при температуре выше 100° С и самой молекулы воды) и, тем самым, освобождение глубоких ловушек, изменение состава носителей заряда (H_3O^+ , OH^- и др.) и их траекторий в объеме. Проводится аналогия между температурным поведением ε , σ , τ_{μ} , j и γ в «пороговых» точках, имеющих характерный одиночный резонансный пик, и дипольным резонансом фотопоглощения в кластерах металлов Ag, Mg и Sm, проявляющаяся в уширении резонанса, расщеплении одиночного пика и образовании однодоменного кристалла $ATGS+Cr^{3+}$ (0,06 масс.% Cr). Мы также обсуждаем возможное возникновение коллективных ядерных возбуждений при облучении образца фотонами или возникновение внутреннего электрического поля смещения E_{dp} при внезапном охлаждении или нагревании образца. Рассмотрено запутывание фотонов по поляризации.

Ключевые слова: гигантский дипольный резонанс, дискретные уровни энергии двухъямного потенциала, диэлектрическая проницаемость и проводимость, когерентные коллективные возбуждения ядер, расщепление резонансных максимумов ε , σ и времени релаксации проводимости τ_u , спиновое поле вероятностей.

Новик Ольга Дмитриевна – студентка 6 курса, ФГБОУ ВО «Московский государственный университет имени М.В. Ломоносова»

Гаврилова Надежда Дмитриевна – д.ф.-м.н., ФГБОУ ВО «Московский государственный университет имени М.В. Ломоносова»

Малышкина Ольга Витальевна – д.ф.-м.н., профессор, профессор кафедры компьютерной безопасности и математических методов управления ФГБОУ ВО «Тверской государственный университет»

Olga D. Novik – 6th vear student, M.V. Lomonosov Moscow State University

Nadezhda D. Gavrilova – Dr. Sc., Professor, M.V. Lomonosov Moscow State University

Olga V. Malyshkina – Dr. Sc., Professor, Full Professor, Department of Computer Security and Mathematical Control Methods, Tver State University

Поступила в редакцию/received: 11.08.2024; после рецензирования/revised: 17.09.2024; принята/ассерted 18.09.2024.